

Detection and Localization of Radiotherapy Targets by Template Matching

H. Mostafavi, A. Sloutsky, and A. Jeung*

Abstract— Radio opaque fiducials are implanted in tumors for the purpose of tracking the target motion using X-ray projections during radiation therapy dose delivery. In this paper we describe and evaluate a novel method based on template matching for detection and localization of arbitrary shaped fiducials. Segmentation methods are not adequate for these fiducials because their appearance in online X-ray projections can vary greatly as a function of imaging angle. The algorithm is based on using the planning CT image to generate templates that correspond to the imaging angles of the online images. We demonstrate successful tracking of complex shape fiducials in clinical images of lung and abdomen. We also validate the algorithm by comparing the results with a segmentation approach for one case in which the fiducials could be tracked by both methods. We also show how by adaptive thresholding of the match scores, we can control the false detection rate.

I. INTRODUCTION

IN this paper we introduce a novel, image-based fiducial tracking method that uses templates generated from a planning computed tomography (CT) image. We demonstrate successful detection and tracking of fiducials using clinical images of tumor sites in abdomen and lung. Stereotactic body radiotherapy (SBRT) of tumors in lung and abdomen is now a common treatment modality. This type of treatment requires high targeting precision and intrafraction monitoring of the tumor motion during radiation dose delivery. Modern radiation therapy machines are equipped with gantry-mounted X-ray imagers that can be used for real-time image guidance during radiation delivery at various gantry rotation angles. However, because of low contrast and overlaying structures, tumor visibility in an X-ray image can be low and greatly change as a function of the imaging angle. Radio-opaque markers are therefore implanted in or near the target volume in anatomical sites that are subject to motion during treatment. These include lung, liver and pancreas, which move with respiration, and prostate, which is subject to transient drifts and excursions. The invasiveness and safety risk of implanting fiducials has been reduced by recent development of new fiducial types and implanting procedures. The majority of these new markers are spatially extended and flexible instead of having the simple shapes of gold cylinders or spherical BBs, the main advantage being the reduced chance of migration because they are designed to engage the surrounding tissue. Because of tissue variability, some of these markers can assume arbitrary shapes in 3D space once implanted. Since during treatment the images are acquired from varying

angles, tracking of the fiducials can be a challenge because of their variable 2D appearance.

We have developed a new algorithm, based on template matching, that can track such irregular shape markers from any imaging angle. It uses a set of templates generated *a priori* from the 3D CT image acquired for treatment planning. The templates are digitally constructed by forward projection of the CT voxel values, while simulating all imaging angles that are expected to be encountered during treatment. In order to track the fiducial in a treatment image, the template with corresponding imaging angle is chosen from the set of digitally constructed templates. Target detection rate and tracking accuracy depend on the quality of the CT image. Clinical planning CT images usually have approximately 1 mm pixel size in trans-axial slices, while the slice spacing is chosen according to specific practices of each clinic, typically ranging from around 1 mm to 3 mm. While a slice spacing of 2 mm or less is recommended for robust tracking results, 3 mm slice spacing has also been shown to work for larger fiducials.

The template-based approach has several key advantages over the segmentation-based algorithms previously used for fiducial tracking (for example Cho et al.¹). These include: a) With templates, a single algorithm addresses different target types, including arbitrary shaped fiducials and a semi rigid formation of such fiducials implanted within roughly 20 mm or less from each other. b) The template embodies all parameters that define the target such as marker count, shape and dimensions; it does not require the separate specification of each of these parameters as required for segmentation. c) The tracked point is uniquely defined in 3D space because a fixed volume of interest (VOI) is used to construct all the templates. In segmentation, the center of mass of the segmented marker is used as the track point. Because of changing appearance of the target from image to image, the 2D centroid can shift and therefore may not represent the image of a unique point in 3D space. d) In template matching, the target “detected or not detected” decision is made by thresholding a single decision variable derived from the set of match scores produced in each matching attempt. This variable quantifies how much the peak match score stands out relative to the lower scores corresponding to other offsets of template relative to the search image. This allows easy control of false detection rate by using an adaptive threshold that is based on the value of match scores outside the candidate peak vicinity. Segmentation-based algorithms, on the other hand, require thresholding of multiple parameters in order to decide whether the target is present in the search region; there is no easy method to relate these multiple thresholds to a false detection rate.

All authors are with Varian Medical Systems, Inc., Palo Alto, CA 94304, USA, (contact email hassan.mostafavi@varian.com)

While template matching with synthesized templates has been used in previous fiducial tracking work, creating fiducial templates from planning CT is novel. Shirato *et al.*² used template matching to track a fiducial implanted in lung in real time using a set of stereo fluoroscopic imagers. However, the fiducial was spherical and appeared the same from different imaging angles. It was tracked using synthesized isotropic templates that matched the expected sphere size. Spherical BBs however are no longer used much in lung since they are more likely to dislodge from the initially implanted position.

Poulsen *et al.*³ investigated a method to synthesize templates for arbitrary shaped fiducials using the X-ray projections acquired prior to each treatment. This semi automatic method segments the fiducial and associates the points on the fiducial as seen in a limited number of projections, thus enabling triangulation to form a 3D model of the points on the fiducial, which is in turn used to create templates corresponding to different viewing angles. The applicability of this method may be limited because it requires user input.

II. METHODS AND MATERIALS

A. The Algorithm

Figure 1 shows the overall block diagram of the algorithm. The main blocks are template generation and template matching, followed by analysis of the match score surface for detection and localization of the target.

In order to generate the template from a CT image for a given X-ray source rotation angle, first we need to specify a volume of interest (VOI) around the set of fiducials. Then the template is generated by forward projection of the voxels inside the VOI, using the imaging geometry corresponding to the simulated source angle. Multiple fiducials implanted close to each other can be grouped to form a single set of templates. In order to demonstrate the ability to track from all gantry angles, we generated CT-based templates for 120 simulated gantry angles spaced at 3 degrees, thus covering the 360-degree full rotation.

Detection and localization of a target is performed by calculating a measure of similarity, called the match score, between the template and the online projection at different offsets over a search region of interest (ROI). The search ROI is centered at the expected target position, and its dimensions are defined by the motion margin expected in each direction. The choice of a particular similarity measure as a match score depends on imaging modality and expected differences between the template and the online image. Normalized cross correlation and mutual information are two possible methods to generate a match score. Mutual information performs well when geometric patterns are consistent between the images but there are random contrast differences, including contrast reversals. This can occur mostly when the template and the online image correspond to different modalities, e.g., when matching PET or MRI to CT images. We used normalized cross correlation, which is computationally faster than mutual information, to compute the match score since in our data both the template and the online image are generated by X-rays.

Calculating the match score at different pixel offsets produces the match score surface defined over the search region, an example of which is shown in Figure 1. The peak of the surface indicates a possible match with the target in the online image. The “sidelobes” are the values of the match score away from the peak vicinity, i.e., non-target locations in the search region. Whether or not a peak corresponds to the location of a target depends on how much it stands out relative to the sidelobes. Therefore the decision variable that is compared with a threshold is the peak-to-sidelobe ratio (PSR), which is defined as the peak value divided by the standard deviation of the sidelobes. This implies an adaptive threshold that is a constant multiple of the standard deviation of the sidelobes, hence keeping the false detection rate constant.

B. Tests on Clinical Images

The overall method was implemented as two research software applications, one for template generation and one for template matching. These were tested on a number of patient datasets with a variety of single and multiple markers. All clinical test images had been acquired using the onboard X-ray imaging system of either TrilogyTM or TrueBeamTM radiotherapy machines (Varian Medical Systems, Inc., Palo Alto, CA 94304). The digital flat panel X-ray imager was configured such that the effective pixel size at target location is 0.259 mm. Most test cases consisted of the projection sets acquired before treatment for the purpose of cone beam CT (CBCT) imaging for patient setup. Other test cases used intrafraction X-ray projection sets acquired for the purpose of target position monitoring. The fiducials were tracked in the image sequence of each test set. In addition to track point coordinates, sample PSR values within the tracking search ROIs were also recorded. Three representative test cases were selected for presentation here.

Figure 2a shows sample CBCT projection images of VisicoilTM (RadioMed Corp., Tyngsboro, MA 01879) fiducials acquired from different directions.

Figure 3a shows another CBCT case with 2 Visicoils in the gastro-esophageal (GE) junction, one coiled up and one almost coiled. In this particular case we tracked these fiducials in the CBCT projection sequence using two methods, segmentation and template matching. We validated the template matching approach by comparing the pixel domain tracks of the two methods.

Figure 4a shows two fiducials of another type, SuperLock BandTM (SuperDimension, Minneapolis, MN 55441), implanted next to each other in lung. These are intrafraction X-ray projections acquired for the purpose of target position monitoring.

III. RESULTS

We successfully tracked the fiducials in a number of CBCT and intrafraction image sets by applying the template matching algorithm using templates generated from the corresponding plan CT images. The results for the three selected cases are as follows.

Sample templates generated from plan CT with corresponding angles are shown in Figures 2b, 3b and 4b.

The slice spacing of the planning CT for these three cases was 2.5mm, 2.5mm and 3mm respectively.

Figures 2c, 3c, and 4c show the pixel domain track coordinates for these three cases. The horizontal axis shows the imaging angle of the gantry-mounted X-ray imager. The range of sample PSR values recoded during tracking was 9.5 to 11.1 for pancreas, 4.4 to 7.4 for GE junction, and 3.9 to 4.6 for the lung case in which the planning CT has the larger 3mm slice spacing. Notice the staircase distortion of the template in the lung case with large CT slice spacing which is partially responsible for the lower PSR values.

For the GE junction case in Figure 3, the fiducials were tracked by a segmentation method in addition to template matching. In this method, the centroid of each fiducial is tracked by segmentation and the midpoint is reported as the track point. The tracking trajectories of the two methods are plotted on the same graph in Figure 3c. The RMS pixel difference calculated over the whole trajectory is equal to 0.67 pixels.

IV. DISCUSSION

The pixel-domain tracking trajectories obtained by template tracking from CBCT projection sequences can be used to generate the 3D trajectory of the fiducial using the sequential stereo tracking algorithm (Mostafavi *et al.*⁴). This trajectory can then be used to optimize the daily patient setup for intrafraction motion management using, for example, beam gating.

The methods presented here are also applicable to the images produced by the treatment beam using the megavoltage (MV) imager onboard linear accelerators (also called electronic portal imager or EPID). For most treatment types, the beam shaping multi-leaf collimator (MLC) leaves move during dose delivery. Therefore, part or all of the fiducials may be obscured in the MV image for some periods of time. Since the leaf positions are known *a priori* for any acquired image, a modified version of the algorithm can mask out the pixel areas obscured by the MLC from the template matching calculation. This can allow tracking of the fiducials even when they are only partially visible in an MV image.

FIGURES

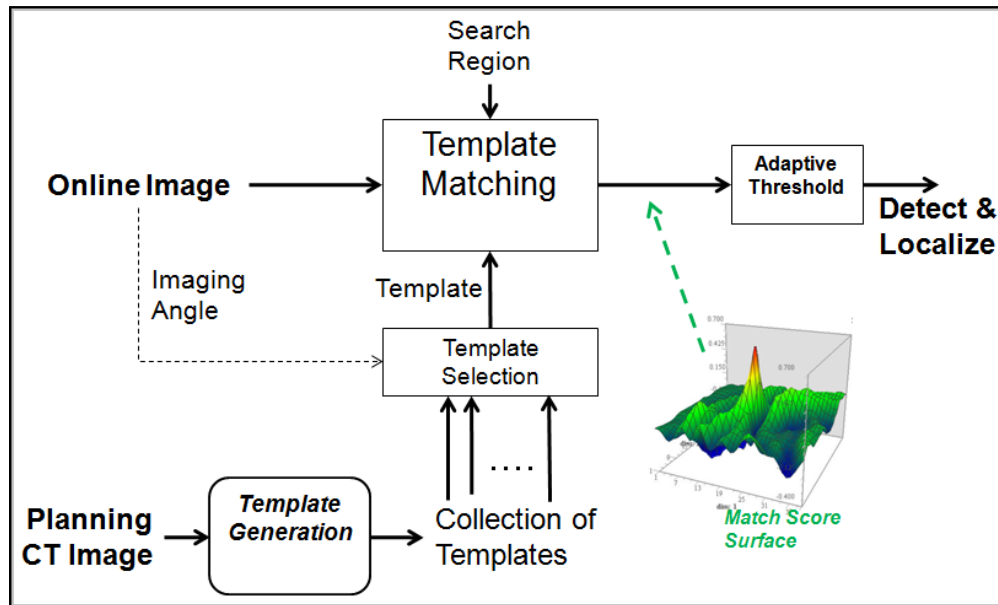


Figure 1. Block diagram of template matching algorithm.

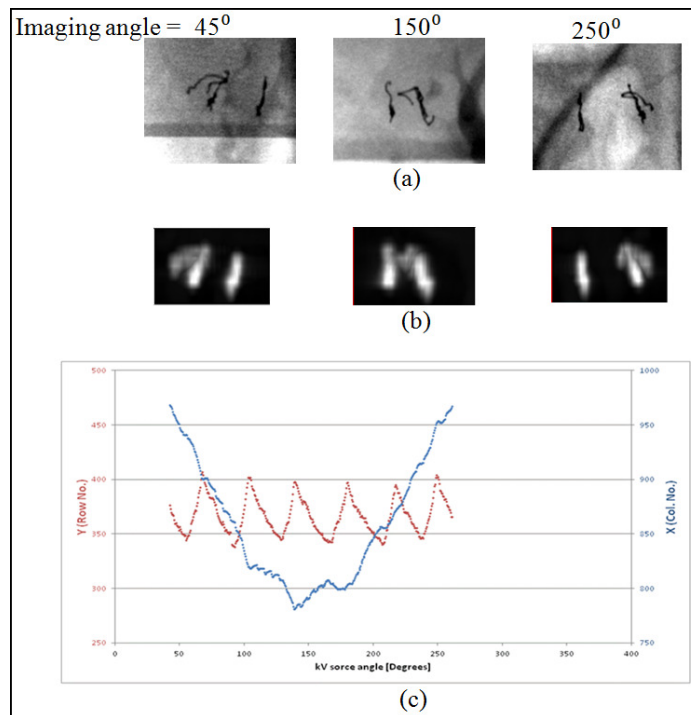


Figure 2. Multiple Visicoils™ in pancreas. (a) Sample online projections (image polarity reversed in CBCT projections); (b) Templates generated from plan CT image, slice spacing = 2.5mm; (c) Pixel-domain track coordinates as a function of the imaging angle; Range of sample PSR values: 9.5 to 11.1.

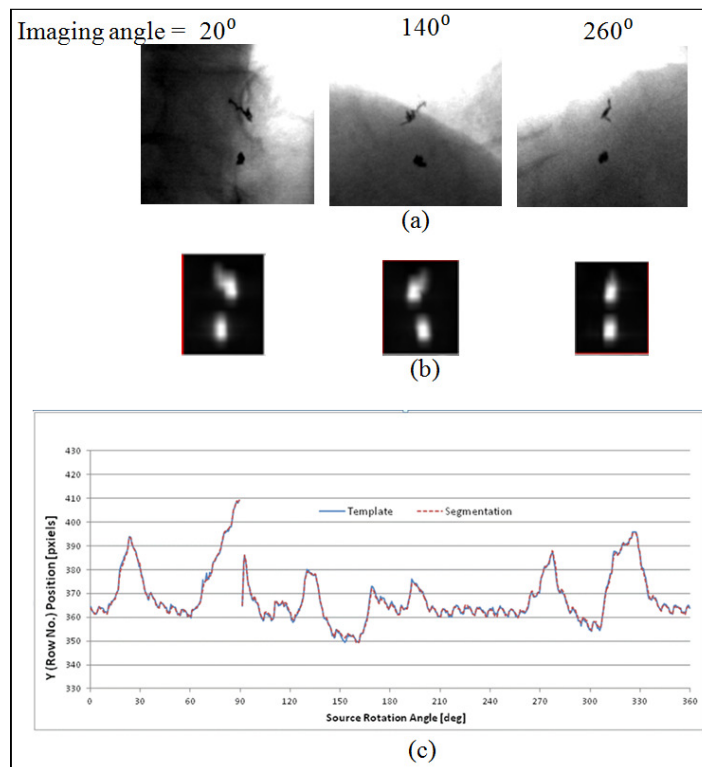


Figure 3. Two Visicoils™ in GE junction. (a) Sample online projections (image polarity reversed in CBCT projections); (b) Templates generated from plan CT image, slice spacing = 2.5mm; (c) Pixel-domain row (longitudinal) position as a function of the imaging angle for both segmentation and template matching; RMS difference between two methods = 0.67 pixels; Range of sample PSR values: 4.4 to 7.4.

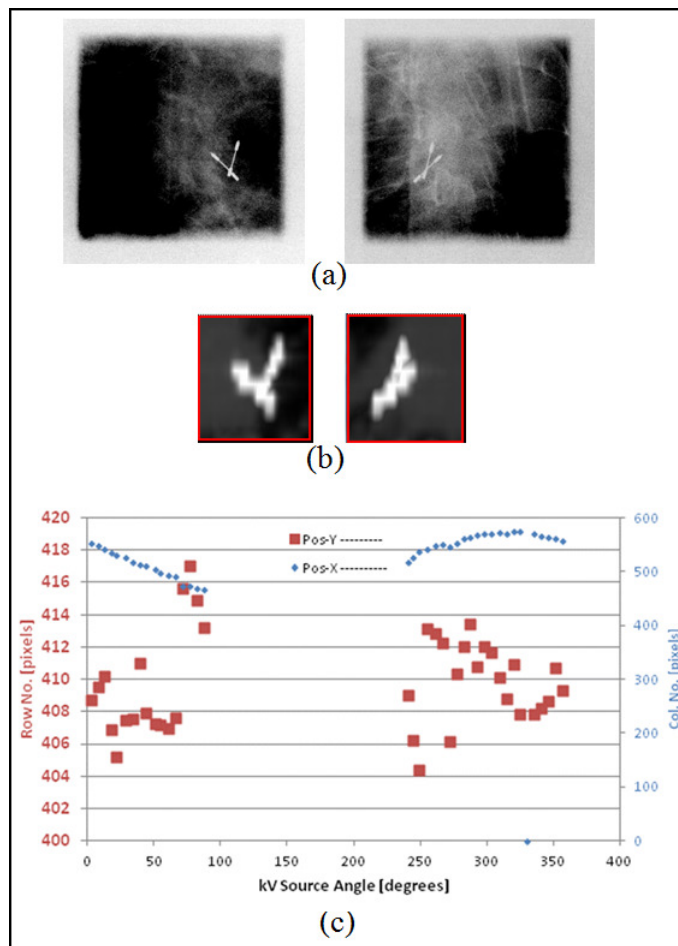


Figure 4. Two SuperLock™ Bands in lung. (a) Sample intrafraction projections; (b) Templates generated from plan CT image, slice spacing = 3mm; (c) Pixel-domain track coordinates for various imaging angles; Range of sample PSR values: 3.9 to 4.6

V. CONCLUSION

Template matching extends the automation of fiducial detection and localization to arbitrary shaped fiducials that are now more commonly used for image guided radiation therapy. The required templates can be successfully generated from a planning CT image.

ACKNOWLEDGMENT

The authors thank Memorial Sloan Kettering Cancer Center and University of Alabama Cancer Center for providing the clinical images used in this work.

REFERENCES

- [1] B. Cho, P. R. Poulsen, A. Sloutsky, A. Sawant, P. J. Keall, "First demonstration of combined kV/MV image-guided real-time DMLC target tracking," *Int J Radiat Oncol Biol Phys.* 2009 July 1; 74(3): 859–867. doi:10.1016/j.ijrobp.2009.02.012.
- [2] H. Shirato, S. Shimizu, T. Kunieda, K. Kitamura, M. Van Herk, K. Kagei, T. Nishioka, S. Hashimoto, K. Fujita, H. Aoyama, K. Tsuchiya, K. Kudo, K. Miyasaka, "Physical aspects of a real-time

tumor-tracking system for gated radiotherapy," *Int. J. Radiation Oncology Biol. Phys.*, Vol. 48, No. 4, pp. 1187–1195, 2000.

- [3] P. R. Poulsen, W. Fledelius, P J Keall, E. Weiss, J. Lu, E. Brackbill, G. D. Hugo, "A method for robust segmentation of arbitrarily shaped radiopaque structures in cone-beam CT projections," *Med. Phys.* **38**, 2151 (2011)
- [4] H. Mostafavi, A. Sloutsky, A. Jeung, "Tracking 3D trajectory of internal markers using radiographic sequential stereo imaging: estimation of breathing motion," *Med. Phys.* **37**, 3430 (2010)